Achieving the depairing limit along the *c* axis in $Fe_{1+y}Te_{1-x}Se_x$ single crystals

Yue Sun,[1,*] Haruka Ohnuma,[1] Shin-ya Ayukawa,[2] Takashi Noji,[3] Yoji Koike,[3] Tsuyoshi Tamegai,[4] and Haruhisa Kitano[1,†]

[1]*Department of Physics and Mathematics, Aoyama Gakuin University, Sagamihara 252-5258, Japan*
[2]*Research Institute for Interdisciplinary Science, Okayama University, Okayama 700-8530, Japan*
[3]*Department of Applied Physics, Tohoku University, Sendai 980-8579, Japan*
[4]*Department of Applied Physics, The University of Tokyo, Tokyo 113-8656, Japan*

(Received 2 November 2019; revised manuscript received 21 March 2020; accepted 1 April 2020; published 27 April 2020)

We report achievement of a depairing current limit along the *c* axis in $Fe_{1+y}Te_{1-x}Se_x$ single crystals. A series of crystals with T_c ranging from 8.6 K to 13.7 K (different amounts of excess Fe, *y*) were fabricated into *c*-axis bridges with a square-micrometer cross-section. The critical current density, J_c, was directly estimated from the transport current-voltage measurements. The transport J_c reaches a very large value, which is about one order of magnitude larger than the depinning J_c, but comparable to the calculated depairing $J_c \sim 2 \times 10^6$ A/cm^2 at 0 K, based on the Ginzburg-Landau (GL) theory. The temperature dependence of the depairing J_c follows the GL theory [$\propto(1\text{-}T/T_c)^{3/2}$] down to $\sim$0.83 T_c, then increases with a reduced slope at low temperatures, which can be qualitatively described by the Kupriyanov-Lukichev theory. Our study provides a route to understand the behavior of depairing J_c in iron-based superconductors in a wide temperature range.

DOI: 10.1103/PhysRevB.101.134516

I. INTRODUCTION

Iron chalcogenide superconductors have attracted much attention because of the discovery of high-temperature superconductivity. Although the superconducting (SC) transition temperature, T_c, in FeSe is only 9 K [1], it can be easily enhanced to 14 K by Te substitution [2], up to 37 K under pressure [3] and over 40 K by intercalating spacer layers [4]. More interestingly, the monolayer of FeSe grown on $SrTiO_3$ shows a large $T_c \sim 65$ K [5]. $Fe_{1+y}Te_{1-x}Se_x$ is unique in structural simplicity, consisting of only FeTe/Se layers, which is favorable for probing the SC mechanism. Recently, a topological surface superconductivity [6,7] and a possible Majorana bound state have been observed [8,9], which makes $Fe_{1+y}Te_{1-x}Se_x$ a high-temperature topological superconductor. On the other hand, its high upper critical field ($\sim$50 Tesla) and a less toxic nature compared with iron pnictides suggest that $Fe_{1+y}Te_{1-x}Se_x$ are also favorable to applications. Until now, the SC tapes with the transport critical current density, J_c, over 10^6 A/cm^2 under self-field and over 10^5 A/cm^2 under 30 T at 4.2 K have already been fabricated [10].

The transport J_c determined by the depairing process of Cooper pairs, called depairing J_c, is crucial for the study of the SC mechanism because it directly provides information on the critical velocity of superfluids, and the magnitude as well as the symmetry of the SC gap [11]. The depairing process occurs when the kinetic energy of the supercurrent exceeds the condensation energy ($\propto$SC gap) [11,12]. However, it is difficult to be achieved since the vortex flow occurs, preceding the depairing at much smaller current density. The critical current density determined by the vortex flow, which occurs when the Lorentz force exceeds the pinning force of vortex, is usually called depinning J_c [12,13]. The depinning J_c obtained from the magnetic hysteresis loops (MHLs) by using the Bean model [14] is mainly determined by the defects, disorders, and the geometry of the samples [13]. On the other hand, J_c can be also obtained from the direct transport measurements on thin films [15,16]. The small thickness of thin films allows us to reach the critical limit by applying not-so-large current. However, single-crystalline thin films without weak links are hard to fabricate due to the presence of grain boundaries and twin boundaries from the growth technique [17,18].

To achieve the depairing J_c, a direct transport current-voltage (I-V) measurement on a single crystal is required. However, it is very difficult for bulk samples to achieve this limit since an extremely large current is needed. To solve this problem, a microfabrication technique is used to reduce the size of the crystal to micrometer or submicrometer scale [19–29]. Until now, studies on the depairing J_c have been mainly performed on low-T_c superconductors, especially at low temperatures [19–22,24,25,30]. For iron-based superconductors (IBSs), the depairing J_c has been probed on the microfabricated $Ba_{1-x}K_xFe_2As_2$ single crystal with current flowing in the *ab* plane [29]. Nonetheless, it was only performed at temperatures close to T_c due to the extremely large in-plane depairing J_c. The depairing J_c for $Ba_{1-x}K_xFe_2As_2$ is found to follow the prediction of the Ginzburg-Landau (GL) theory at temperatures close to T_c [29]. However, the behavior of the depairing J_c at low temperatures for IBSs still remains unknown.

*sunyue@phys.aoyama.ac.jp
†hkitano@phys.aoyama.ac.jp

 ©2020 American Physical Society

TABLE I. Depairing current density for typical iron-based superconductors, calculated by $J_{dp}^{GL} = c\phi_0/12\sqrt{3}\pi^2\xi(0)\lambda(0)^2$, where c is the speed of light, ϕ_0 is the flux quantum, $\xi(0)$ is the coherence length at 0 K, and $\lambda(0)$ is the penetration depth at 0 K, respectively. Here, we should note that the anisotropies of some IBSs estimated from penetration depth λ_c/λ_{ab} and coherence length ξ_{ab}/ξ_c are different at temperatures much below T_c [31]. Therefore, we prefer to use the experimental values of λ and ξ for the calculations.

	$\lambda_{ab}(0)$ (μm)	$\lambda_c(0)$ (μm)	$\xi_{ab}(0)$ (nm)	$\xi_c(0)$ (nm)	$J_{dp}^{GL}(ab)$ (A/cm^2)	$J_{dp}^{GL}(c)$ (A/cm^2)
$FeTe_{1-x}Se_x$	0.49 [32]	1.32 [32]	2.8 [33]	3 [33]	1.5×10^7	2.0×10^6
FeSe	0.45 [34]	1.1 [35]	4.3 [36]	2.9 [37]	1.2×10^7	2.9×10^6
$NdFeAsO_{1-x}F_x$	0.2 [31]	3.7 [31]	2.3 [38]	0.26 [38]	1.1×10^8	2.8×10^6
$Ba_{1-x}K_xFe_2As_2$	0.25 [31]	1.8 [31]	2.2 [39]	2.2 [39]	7.4×10^7	1.4×10^6
$Ba(Fe_{1-x}Co_x)_2As_2$	0.2 [40]	1.0 [40]	2.4 [41]	1.2 [41]	1.1×10^8	8.4×10^6
$BaFe_2(As_{1-x}P_x)_2$	0.2 [42]	–	3.2 [43]	1.3 [43]	7.9×10^7	–
$K_xFe_2Se_2$	0.29 [44]	–	2.3 [45]	1.4 ∼ 2.3 [45]	5.2×10^7	–
LiFeAs	0.21 [46]	–	4.8 [47]	1.7 [47]	4.8×10^7	–

To reveal the behavior of the depairing J_c at lower temperatures, we turn eyes on the J_c along the c axis. As summarized in Table I, the theoretical depairing J_c along the c axis for IBSs is about one order smaller than that in the ab plane due to the larger penetration depth λ_c, which is advantageous for achieving the depairing limit. Until now, the J_c along the c axis in microfabricated single crystals has already been studied in IBSs $(V_2Sr_4O_6)Fe_2As_2$ and Sm/PrFeAs(O,F). However, the depairing limit is not achieved because of the possible formation of intrinsic Josephson junctions [26,48,49]. In this study, we focus on the $Fe_{1+y}Te_{1-x}Se_x$ single crystals, whose depinning J_c for both $H \parallel c$ and $H \parallel ab$ are typically 3×10^5 A/cm^2 at 2 K [50,51]. When the current is flowing in the ab plane, the depairing J_c is estimated as 1.5×10^7 A/cm^2 (see Table I). On the other hand, when the current is flowing along the c axis, the depairing J_c is estimated as 2.0×10^6 A/cm^2 (see Table I), which is more suitable for probing the depairing J_c at low temperatures.

In this paper, we successfully achieve the depairing limit in $Fe_{1+y}Te_{1-x}Se_x$ single crystals by fabricating narrow bridges along the c axis. The obtained transport J_c is about one order of magnitude larger than the depinning J_c, indicating the obtained J_c is the depairing J_c. Besides, the temperature dependence of the depairing J_c is studied down to ∼0.3 T_c, which can be qualitatively described by the Kupriyanov-Lukichev (KL) theory.

II. EXPERIMENT

$Fe_{1+y}Te_{1-x}Se_x$ ($x = 0.2$, 0.3, and 0.4) single crystals were grown by slow cooling method [52,53]. All the crystals show platelike morphology and can grow up to the size of a centimeter. Only the (00l) peaks are observed in the single crystal x-ray diffraction, suggesting that the crystallographic c axis is perfectly perpendicular to the plane of the single crystal [54]. Crystal composition is evaluated by inductively coupled plasma atomic emission spectroscopy, which confirms that the actual Se-doping level is very close to the nominal one [52,54]. On the other hand, the as-grown crystals usually contain some amount of excess Fe (represented by y, ∼0.14 in the $Fe_{1+y}Te_{0.6}Se_{0.4}$ single crystal [55]) residing in the interstitial sites of the Te/Se layer. The excess Fe was removed and its amount was tuned by both the postannealing and electrochemical reaction method, as reported in our previous publications [55,56]. Together with the removal of excess Fe, T_c is found to be spontaneously increased [55,57]. In the fully annealed crystals, the excess Fe was totally removed as confirmed by scanning tunneling microscopy measurements [9,55]. By these methods, a series of single crystals with different T_c, i.e., different amount of excess Fe, were prepared. More details about the crystal, excess Fe, and the basic properties can be seen in a recent review paper [58].

The c-axis bridge, as shown schematically in Fig. 1(b), was fabricated by using the focused ion beam (FIB) technique [60–62]. The single crystal was first cleaved into a slice with a thickness smaller than 10 μm, and fixed on a sapphire substrate. Then the central part of the crystal was necked down to a length of 5 ∼ 10 μm and a width of ∼1 μm from the top by FIB. The necked part was further fabricated into two separated slits with a typical overlap of 100 ∼ 200 nm, which will enforce the current to flow along the c axis in the bridge region as marked by the rectangular frame in Fig. 1(c). With such a structure, the critical current density of the device is determined by the c-axis bridge since the other parts of the crystal have much larger cross areas. The scanning ion microscopy image of a typical c-axis bridge structure is shown in Fig. 1(a). The cross-section areas ($w \times h$) of the bridges together with the value of T_c are listed in Table II.

Resistance measurements were performed by a standard four-probe method. The I-V measurements were performed below T_c by applying two kinds of pulse currents to the c-axis bridge. In the first method, the bias current was linearly swept

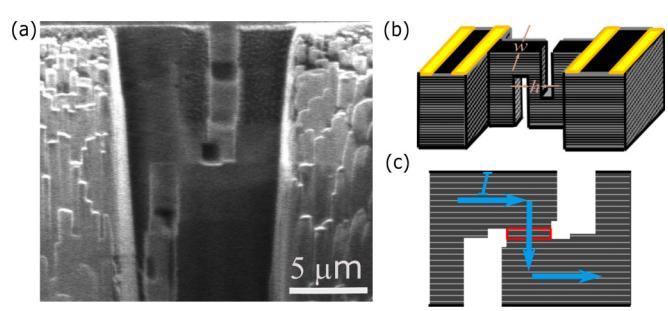

FIG. 1. (a) The scanning ion microscopy images of the fabricated c-axis structure in $Fe_{1+y}Te_{1-x}Se_x$ single crystal. Schematic drawing of (b) the bridge structure and (c) the current-flowing path along the c-axis bridge.

TABLE II. Cross-section areas ($w \times h$) of the fabricated c-axis bridges. Λ is the Pearl length calculated by $2\lambda_c^2/h$ [59], where λ_c is the penetration depth along c axis, ~1.6 μm at 5 K [32].

T_c (K)	w (μm)	h (μm)	Λ (μm)
8.6	2.0	1.1	4.7
8.8	2.0	1.1	4.7
9.3	1.4	1.3	3.9
9.5	1.4	1.0	5.1
10.9	0.8	1.2	4.3
11.9	1.7	1.5	3.4
12.8	1.4	0.9	5.7
13.7	3.4	1.0	5.1

up and down through a standard resistance (1 kΩ) by using an arbitrary wave-form generator (Agilent 33220A). The width of such a ramped current pulse is 5 ms and the repetition period is 143 ms. In the second method, the pulse current was applied by using a Keithley Delta Pulse System. Rectangular 100 μs current pulses were passed through the sample at 3 s intervals (duty ratio ~3.3×10^{-5}) to avoid heating effect. The voltage drop across the bridge was integrated for 55 μs. To avoid damage to the c-axis bridge, the pulse current was stopped when the voltage reaches the threshold value of 30 μV.

Here, we point out that the resistance measurements probe the region intervening between the two voltage contacts on the crystal, where the narrow bridge and other crystalline parts are included. On the other hand, the I-V measurements performed below T_c probe only the part of the microfabricated narrow bridge. Thus, the effects of sample inhomogeneity in the resistance measurements should be carefully distinguished with those in the I-V measurements, as will be discussed in the next section.

III. RESULTS AND DISCUSSION

Figures 2(a) and 2(b) show the temperature dependence of the resistance for two typical microfabricated crystals with T_c = 10.9 K and 13.7 K, respectively. The value of T_c is determined by the zero resistance. According to our previous studies, the increase of T_c is due to the reduction of excess Fe [55,56]. The well-annealed crystal without excess Fe (e.g., the crystal with T_c = 13.7 K) shows a sharp SC transition width as shown in Fig. 2(b), while the crystals with some amount of excess Fe left show a slightly broader transition [e.g., the crystal with T_c = 10.9 K shown in Fig. 2(a)]. This transition suggests the slight inhomogeneity, which is derived from the residual excess Fe or the small damage due to the FIB fabrication in the narrow bridge [61,63]. However, as described in detail below, such a broad transition does not affect the determination of the transport J_c in the I-V measurements performed below T_c.

The I-V curves for the two samples measured at different temperatures are presented in Figs. 2(c) and 2(d). The I-V characteristics in Fig. 2(c) were measured by using the first method. The critical current, I_c, was simply determined by the current where the voltage abruptly jumps from zero to a finite value. When the current sweeps up and down, hysteresis

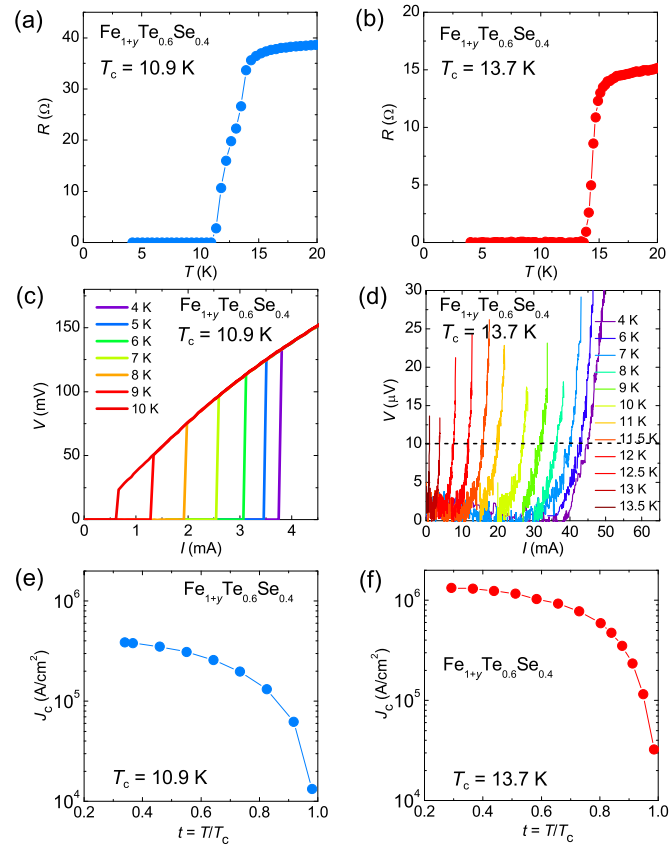

FIG. 2. Temperature dependence of the resistance measured at zero field for the microfabricated (a) $Fe_{1+y}Te_{0.6}Se_{0.4}$ with T_c = 10.9 K and (b) 13.7 K, respectively. (c), (d) The corresponding I-V curves measured at different temperatures for the two samples. (e), (f) Temperature dependence of the J_c for the two samples estimated from (c), (d).

loops in the I-V characteristics are observed, which are due to the Joule heating effect (see Supplemental Material [64]). Such heating effects only occur when the applied current exceeds the critical current, which will not affect the determination of I_c. To minimize the degradation of I_c by repeating the relatively large pulse current, the I-V characteristics in Fig. 2(d) was measured by using the second method. A criterion of 10 μV [indicated as the dashed line in Fig. 2(d)] was used to define the critical current. In both methods, we emphasize that the I_c is determined by the SC current passing through a minimum cross-sectional area, S, of the bridge in the zero-resistance state below T_c, since the SC current flows avoiding the non-SC region in the bridge. Thus, the SC transition region showing a finite resistance above T_c is clearly out of the scope of the I_c measurements performed below T_c. Furthermore, although the effective value of S can be changed by the secondary SC transition of the non-SC region in the bridge, we confirmed that the effective S for both samples was independent of temperature below T_c, based on the following two facts. One is the smooth increase of J_c given by I_c/S shown in Figs. 2(e) and 2(f). The other is the excellent agreement between the scaled J_c for both crystals with T_c = 10.9 K and 13.7 K (see Fig. 3). Thus, we conclude that the broader SC transition observed in Fig. 2(a) has no influence on the behavior of J_c.

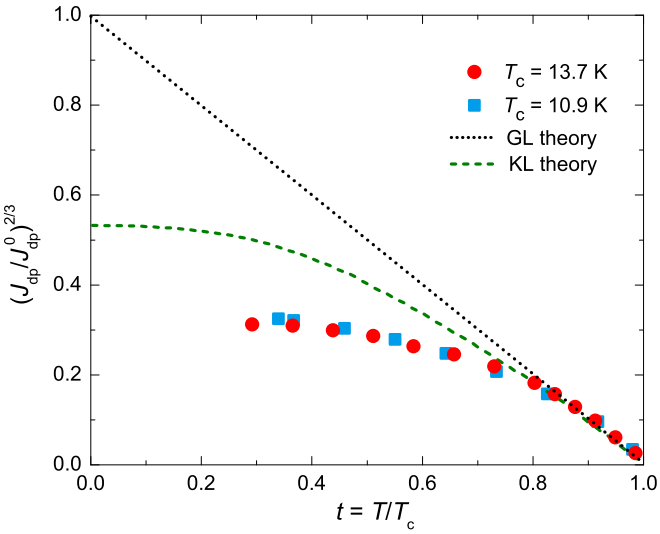

FIG. 3. Reduced temperature (t=T/T_c) dependence of the depairing current density, normalized to the extrapolated value J^0_{dp}, along c axis for the $Fe_{1+y}Te_{0.6}Se_{0.4}$ with T_c = 13.7 K and 10.9 K. The dotted and the dashed lines represent the results from the GL theory and KL theory, respectively.

As shown in Figs. 2(e) and 2(f), the values of J_c are obviously enhanced with the increase of T_c. In the crystal with T_c = 13.7 K [see Fig. 2(f)], J_c reaches a very large value $\sim 1.3 \times 10^6$ A/cm^2 at 4 K. This value of the transport J_c is about one order of magnitude larger than the depinning J_c ($\sim 1.3 \times 10^5$ A/cm^2 at 4 K), which has been estimated from the MHLs for both $H \parallel c$ and $H \parallel ab$ [50,51]. On the other hand, the depairing J_c along the c axis given in the GL theory by $J^{GL}_{dp} = c\phi_0/12\sqrt{3}\pi^2\xi_c\lambda_c^2$ is estimated as $\sim 2 \times 10^6$ A/cm^2 using the coherence length $\xi_c(0\text{ K}) \simeq 3.0$ nm [33], and penetration depth $\lambda_c(0\text{ K}) \simeq 1.32$ μm [32]. The calculated $J^{GL}_{dp}(0\text{ K})$ is comparable to our experimental value $\sim 1.3 \times 10^6$ A/cm^2 at 4 K.

In general, the critical current density at zero applied magnetic field is determined by the edge barrier for current-induced vortices, which prevents the vortex from entering the bridge. The edge barrier decreases with increasing the applied current and will be completely suppressed when the current density approaching the critical limit, where the vortex begins to enter the bridge [11]. Theoretically, the depairing current density can be obtained when the transverse dimension of the bridge is made small compared to both the coherence length and the penetration depth [11]. In high-T_c superconductors, the condition is difficult to be fulfilled since their coherence length is too small, typically several nanometers. In practice, the depairing limit can be achieved if the current is homogeneously distributed in the bridge [11,27]. However, the supercurrent tends to pile up at the edges of the bridge because the magnetic flux density is the largest there as the flux lines circle the bridge [11,20]. This effect makes the current density nonuniform. In this case, the vortex begins to enter the bridge from edges when the averaged current density is still much smaller than the depairing limit. In other words, the obtained J_c is much smaller than the depairing J_c.

This effect has been overcome when the width of the bridge (w) is reduced to the Pearl length $\Lambda = 2\lambda^2/h$, where λ is the penetration depth and h is the thickness of the bridge [59]. In this case, the current density is uniformly distributed in the bridge, and the depairing limit can be achieved. Such a method has been successfully applied to achieve the depairing limit in $YBa_2Cu_3O_{7-\delta}$ and $Ba_{0.5}K_{0.5}Fe_2As_2$ [27,29]. In the present paper, the size and the calculated Pearl length Λ for the c-axis bridges are listed in Table II (to directly compare with the experiments which are down to 4 K, the penetration depth at 5 K rather than 0 K is used for calculation.). The width (w) of the bridge is smaller than the Pearl length Λ, and comparable to the λ_c for all the fabricated c-axis bridges, which guarantees the uniform current density. Thus, the large transport J_c observed in the c-axis bridge of $Fe_{1+y}Te_{1-x}Se_x$ single crystal is attributed to the depairing current limit. In the following paragraphs, we use J_{dp} to express the depairing current density.

In the GL theory, J_{dp} close to T_c can be described as a function of the reduced temperature $t = T/T_c$ by the formula $J^{GL}_{dp}(t) = J^{GL}_{dp}(0)(1\text{-}t)^{3/2}$ [11]. To compare our experimental data with the theory, we fit the linear behavior of $J^{2/3}_{dp}$ close to T_c, and extrapolate it to $t = 0$ to extract J^0_{dp} as used in the previous reports [24,25]. The reduced temperature dependencies of the normalized depairing current density $(J_{dp}/J^0_{dp})^{2/3}$ are shown in Fig. 3, together with the theoretical results from the GL theory (dotted line) and KL theory (dashed line) [65]. We find that $(J_{dp}/J^0_{dp})^{2/3}$ for the crystal of $T_c \sim 10.9$ K falls onto an identical curve for the crystal of $T_c \sim 13.9$ K, confirming that J_c is homogeneous in the bridge part in spite of the broader resistive transition. The experimental data follows the GL behavior, which increases linearly with decreasing t down to ~ 0.83 T_c. Then, $(J_{dp}/J^0_{dp})^{2/3}$ gradually deviates from the GL behavior with a reducing slope at lower t. Such saturation behavior was similar to those observed in low-temperature superconductors [20,22,24,25] and can be qualitatively described by the microscopic KL theory, where the J_{dp} was numerically calculated from the Eilenberger equations by assuming that the velocity of supercurrent is proportional to a phase gradient of the SC order parameter [65].

Quantitatively, the values of $(J_{dp}/J^0_{dp})^{2/3}$ are smaller than the theoretical ones at low temperatures. The fact that $(J_{dp}/J^0_{dp})^{2/3}$ of the two $Fe_{1+y}Te_{0.6}Se_{0.4}$ bridges with different T_c almost fall into an identical curve suggests the unified origin of the smaller value rather than the impurity level of the sample. The smaller J_{dp} than the theoretical one has also been observed in the microfabricated $YBa_2Cu_3O_{7-\delta}$ [27] and some Nb thin films [24]. The former one is attributed to the current crowding at the inner corners of the junction between the bridge and electrode, which makes the local current density at the inner corners larger than the averaged one at the center of the bridge [27]. The latter one is discussed to be the heating effect on the contacts, which cause extra vortex flowing [24]. Besides, the GL theory and KL theory are all based on the conventional superconductors with one band structure. A recent theoretical calculation shows that the depairing J_c for the real material should be smaller than that expected from the KL theory due to the broadening of the peaks in the quasiparticle density of states [66]. Moreover, $Fe_{1+y}Te_{1-x}Se_x$ is a multiband system with strong interband

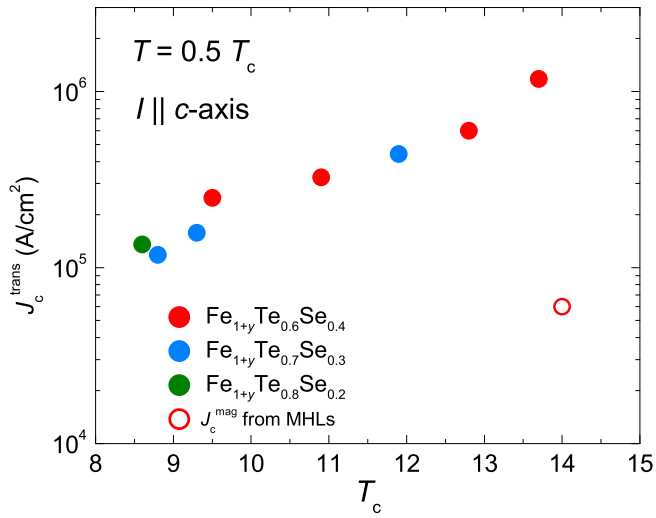

FIG. 4. Evolution of J_c at T=0.5 T_c with T_c for different crystals. The red, blue, and green circles represent the results obtained from the fabricated $Fe_{1+y}Te_{0.6}Se_{0.4}$, $Fe_{1+y}Te_{0.7}Se_{0.3}$, and $Fe_{1+y}Te_{0.8}Se_{0.2}$ single crystals, respectively. The open circle is the self-field J_c estimated from the magnetic hysteresis loops by Bean model [50,51].

scattering [67]. Future efforts of theoretical consideration on the multiband effect may be required to understand the temperature dependence of the depairing J_c property.

To directly observe the evolution of transport J_c with the value of T_c, (i.e., the amount of excess Fe), we summarized the J_c for all the crystals at $T = 0.5\ T_c$, and plotted versus their values of T_c in Fig. 4. It is clear that J_c increases monotonically with T_c independent of the amount of Se. Note that J_c of the crystal with minimum T_c is still larger than the depinning J_c estimated from MHLs (see the open symbol in Fig. 4) [50,51]. It indicates that the depairing current limit is achieved in all the samples. On the other hand, the depairing J_c decreases quickly with the suppression of T_c. Such a strong decrease of depairing J_c cannot be explained by the difference in bridge dimensions, since the sample with the highest J_c has the largest width close to the Pearl length. The decrease of depairing J_c may be due to the effect of excess Fe. Density-functional study shows that the excess Fe is strongly magnetic, providing local moments, which will act as a pair breaker [68]. In addition, the edge barriers in the disordered region around the excess Fe is considered to be weakened, which will cause local suppression of J_c. Our results suggest that removing the excess Fe is crucial for the increase of the current capacity limit as well as the depairing J_c for the $Fe_{1+y}Te_{1-x}Se_x$, which is instructive for other studies on thin films, tapes, and the nanoscale devices such as the single photon detectors and the nanoSQUIDs.

IV. CONCLUSIONS

In conclusion, we investigated the transport critical current density along the c axis in $Fe_{1+y}Te_{1-x}Se_x$ single crystals. A series of crystals containing different amounts of excess Fe with T_c ranging from 8.6 K to 13.7 K were fabricated into c-axis bridges for the transport I-V measurements. J_c reaches a much larger value than the magnetic J_c obtained from MHLs, which is explained by reaching the depairing limit. The depairing J_c follows the GL theory down to ~0.83 T_c, then increases with a reducing slope at lower temperatures, which can be qualitatively described by the KL theory. This work indicates that the depairing current limit of high-T_c superconductors can be explored by fabricating the c-axis narrow bridges. Future efforts on fabricating other IBSs are expected to reveal the common behavior of the depairing J_c in the whole temperature range.

ACKNOWLEDGMENTS

The present work was partly supported by KAKENHI (No. JP20H05164, No. 19K14661, No. 18K03547, No.16K13841, No. 18H05853, and No. 17H01141) from JSPS. FIB microfabrication performed in this work was supported by Center for Instrumental Analysis, College of Science and Engineering, Aoyama Gakuin University.

[1] F. C. Hsu, J. Y. Luo, K. W. Yeh, T. K. Chen, T. W. Huang, P. M. Wu, Y. C. Lee, Y.-L. Huang, Y.-Y. Chu, D. C. Yan, and M. K. Wu, Proc. Nat. Acad. Sci. **105**, 14262 (2008).
[2] B. C. Sales, A. S. Sefat, M. A. McGuire, R. Y. Jin, D. Mandrus, and Y. Mozharivskyj, Phys. Rev. B **79**, 094521 (2009).
[3] S. Medvedev, T. M. McQueen, I. A. Troyan, T. Palasyuk, M. I. Eremets, R. J. Cava, S. Naghavi, F. Casper, V. Ksenofontov, G. Wortmann, and C. Felser, Nat. Mater. **8**, 630 (2009).
[4] M. Burrard-Lucas, D. G. Free, S. J. Sedlmaier, J. D. Wright, S. J. Cassidy, Y. Hara, A. J. Corkett, T. Lancaster, P. J. Baker, S. J. Blundell, and S. J. Clarke, Nat. Mater. **12**, 15 (2013).
[5] S. He, J. He, W. Zhang, L. Zhao, D. Liu, X. Liu, D. Mou, Y. B. Ou, Q. Y. Wang, Z. Li, L. Wang, Y. Peng, Y. Liu, C. Chen, L. Yu, G. Liu, X. Dong, J. Zhang, C. Chen, Z. Xu, X. Chen, X. Ma, Q. Xue, and X. J. Zhou, Nat. Mater. **12**, 605 (2013).
[6] P. Zhang, K. Yaji, T. Hashimoto, Y. Ota, T. Kondo, K. Okazaki, Z. Wang, J. Wen, G. D. Gu, H. Ding, and S. Shin, Science **360**, 182 (2018).
[7] P. Zhang, Z. Wang, X. Wu, K. Yaji, Y. Ishida, Y. Kohama, G. Dai, Y. Sun, C. Bareille, K. Kuroda, T. Kondo, K. Okazaki, K. Kindo, X. Wang, C. Jin, J. Hu, R. Thomale, K. Sumida, S. Wu, K. Miyamoto, T. Okuda, H. Ding, G. D. Gu, T. Tamegai, T. Kawakami, M. Sato, and S. Shin, Nat. Phys. **15**, 41 (2019).
[8] D. Wang, L. Kong, P. Fan, H. Chen, S. Zhu, W. Liu, L. Cao, Y. Sun, S. Du, J. Schneeloch, R. Zhong, G. Gu, L. Fu, H. Ding, and H.-J. Gao, Science **362**, 333 (2018).
[9] T. Machida, Y. Sun, S. Pyon, S. Takeda, Y. Kohsaka, T. Hanaguri, T. Sasagawa, and T. Tamegai, Nat. Mater. **18**, 811 (2019).
[10] W. Si, S. J. Han, X. Shi, S. N. Ehrlich, J. Jaroszynski, A. Goyal, and Q. Li, Nat. Commun. **4**, 1347 (2013).
[11] M. Tinkham, *Introduction to Superconductivity* (Courier Corporation, New York, 1996).
[12] D. Dew-Hughes, Low Temp. Phys. **27**, 713 (2001).
[13] G. Blatter, M. V. Feigel'man, V. B. Geshkenbein, A. I. Larkin, and V. M. Vinokur, Rev. Mod. Phys. **66**, 1125 (1994).

[14] C. P. Bean, Rev. Mod. Phys. **36**, 31 (1964).
[15] J. de Vries, G. Stollman, and M. Gijs, Physica C **157**, 406 (1989).
[16] J. Hänisch, K. Iida, R. Hühne, and C. Tarantini, Supercond. Sci. Technol. **32**, 093001 (2019).
[17] H. Hilgenkamp and J. Mannhart, Rev. Mod. Phys. **74**, 485 (2002).
[18] J. H. Durrell, C.-B. Eom, A. Gurevich, E. E. Hellstrom, C. Tarantini, A. Yamamoto, and D. C. Larbalestier, Rep. Prog. Phys. **74**, 124511 (2011).
[19] A. T. Fiory, A. F. Hebard, and S. Somekh, Appl. Phys. Lett. **32**, 73 (1978).
[20] W. J. Skocpol, Phys. Rev. B **14**, 1045 (1976).
[21] K. Xu, P. Cao, and J. R. Heath, Nano Lett. **10**, 4206 (2010).
[22] J. Romijn, T. M. Klapwijk, M. J. Renne, and J. E. Mooij, Phys. Rev. B **26**, 3648 (1982).
[23] P. Yang and C. M. Lieber, Science **273**, 1836 (1996).
[24] A. Y. Rusanov, M. B. S. Hesselberth, and J. Aarts, Phys. Rev. B **70**, 024510 (2004).
[25] C. Cirillo, A. Rusanov, C. Bell, and J. Aarts, Phys. Rev. B **75**, 174510 (2007).
[26] P. J. W. Moll, R. Puzniak, F. Balakirev, K. Rogacki, J. Karpinski, N. D. Zhigadlo, and B. Batlogg, Nat. Mater. **9**, 628 (2010).
[27] S. Nawaz, R. Arpaia, F. Lombardi, and T. Bauch, Phys. Rev. Lett. **110**, 167004 (2013).
[28] M. Liang, M. N. Kunchur, L. Fruchter, and Z. Li, Physica C: **492**, 178 (2013).
[29] J. Li, J. Yuan, Y.-H. Yuan, J.-Y. Ge, M.-Y. Li, H.-L. Feng, P. J. Pereira, A. Ishii, T. Hatano, A. V. Silhanek, L. F. Chibotaru, J. Vanacken, K. Yamaura, H.-B. Wang, E. Takayama-Muromachi, and V. V. Moshchalkov, Appl. Phys. Lett. **103**, 062603 (2013).
[30] M. N. Kunchur, J. Phys.: Condens. Matter **16**, R1183 (2004).
[31] R. Prozorov, M. Tanatar, R. Gordon, C. Martin, H. Kim, V. Kogan, N. Ni, M. Tillman, S. Bud'ko, and P. Canfield, Physica C **469**, 582 (2009).
[32] M. Bendele, S. Weyeneth, R. Puzniak, A. Maisuradze, E. Pomjakushina, K. Conder, V. Pomjakushin, H. Luetkens, S. Katrych, A. Wisniewski, R. Khasanov, and H. Keller, Phys. Rev. B **81**, 224520 (2010).
[33] H. Lei, R. Hu, E. S. Choi, J. B. Warren, and C. Petrovic, Phys. Rev. B **81**, 094518 (2010).
[34] S. Kasahara, T. Watashige, T. Hanaguri, Y. Kohsaka, T. Yamashita, Y. Shimoyama, Y. Mizukami, R. Endo, H. Ikeda, K. Aoyama, T. Terashima, S. Uji, T. Wolf, H. von Löhneysen, T. Shibauchi, and Y. Matsuda, Proc. Nat. Acad. Sci. **111**, 16309 (2014).
[35] R. X. Cao, J. Dong, Q. L. Wang, Y. J. Yang, C. Zhao, X. H. Zeng, D. A. Chareev, A. N. Vasiliev, B. Wu, and G. Wu, AIP Adv. **9**, 045220 (2019).
[36] H. Lei, R. Hu, and C. Petrovic, Phys. Rev. B **84**, 014520 (2011).
[37] S. I. Vedeneev, B. A. Piot, D. K. Maude, and A. V. Sadakov, Phys. Rev. B **87**, 134512 (2013).
[38] Y. Jia, P. Cheng, L. Fang, H. Luo, H. Yang, C. Ren, L. Shan, C. Gu, and H.-H. Wen, Appl. Phys. Lett. **93**, 032503 (2008).
[39] H. Q. Yuan, J. Singleton, F. F. Balakirev, S. A. Baily, G. F. Chen, J. L. Luo, and N. L. Wang, Nature **457**, 565 (2009).
[40] R. Prozorov and V. G. Kogan, Rep. Prog. Phys. **74**, 124505 (2011).
[41] A. Yamamoto, J. Jaroszynski, C. Tarantini, L. Balicas, J. Jiang, A. Gurevich, D. C. Larbalestier, R. Jin, A. S. Sefat, M. A. McGuire, B. C. Sales, D. K. Christen, and D. Mandrus, Appl. Phys. Lett. **94**, 062511 (2009).
[42] K. Hashimoto, K. Cho, T. Shibauchi, S. Kasahara, Y. Mizukami, R. Katsumata, Y. Tsuruhara, T. Terashima, H. Ikeda, M. A. Tanatar, H. Kitano, N. Salovich, R. W. Giannetta, P. Walmsley, A. Carrington, R. Prozorov, and Y. Matsuda, Science **336**, 1554 (2012).
[43] S. Chong, S. Hashimoto, and K. Kadowaki, Solid State Commun. **150**, 1178 (2010).
[44] D. A. Torchetti, M. Fu, D. C. Christensen, K. J. Nelson, T. Imai, H. C. Lei, and C. Petrovic, Phys. Rev. B **83**, 104508 (2011).
[45] E. D. Mun, M. M. Altarawneh, C. H. Mielke, V. S. Zapf, R. Hu, S. L. Bud'ko, and P. C. Canfield, Phys. Rev. B **83**, 100514(R) (2011).
[46] D. S. Inosov, J. S. White, D. V. Evtushinsky, I. V. Morozov, A. Cameron, U. Stockert, V. B. Zabolotnyy, T. K. Kim, A. A. Kordyuk, S. V. Borisenko, E. M. Forgan, R. Klingeler, J. T. Park, S. Wurmehl, A. N. Vasiliev, G. Behr, C. D. Dewhurst, and V. Hinkov, Phys. Rev. Lett. **104**, 187001 (2010).
[47] J. L. Zhang, L. Jiao, F. F. Balakirev, X. C. Wang, C. Q. Jin, and H. Q. Yuan, Phys. Rev. B **83**, 174506 (2011).
[48] P. J. W. Moll, X. Zhu, P. Cheng, H.-H. Wen, and B. Batlogg, Nat. Phys. **10**, 644 (2014).
[49] H. Kashiwaya, K. Shirai, T. Matsumoto, H. Shibata, H. Kambara, M. Ishikado, H. Eisaki, A. Iyo, S. Shamoto, I. Kurosawa, and S. Kashiwaya, Appl. Phys. Lett. **96**, 202504 (2010).
[50] Y. Sun, T. Taen, Y. Tsuchiya, Q. Ding, S. Pyon, Z. Shi, and T. Tamegai, Appl. Phys. Express **6**, 043101 (2013).
[51] Y. Sun, T. Taen, T. Yamada, Y. Tsuchiya, S. Pyon, and T. Tamegai, Supercond. Sci. Technol. **28**, 044002 (2015).
[52] T. Noji, T. Suzuki, H. Abe, T. Adachi, M. Kato, and Y. Koike, J. Phys. Soc. Jpn. **79**, 084711 (2010).
[53] Y. Sun, T. Taen, Y. Tsuchiya, Z. X. Shi, and T. Tamegai, Supercond. Sci. Technol. **26**, 015015 (2013).
[54] Y. Sun, T. Yamada, S. Pyon, and T. Tamegai, Sci. Rep. **6**, 32290 (2016).
[55] Y. Sun, Y. Tsuchiya, T. Taen, T. Yamada, S. Pyon, A. Sugimoto, T. Ekino, Z. Shi, and T. Tamegai, Sci. Rep. **4**, 4585 (2014).
[56] K. Okada, T. Takagi, M. Kobayashi, H. Ohnuma, T. Noji, Y. Koike, S. Ayukawa, and H. Kitano, Jpn. J. Appl. Phys. **57**, 040305 (2018).
[57] Y. Sun, T. Taen, T. Yamada, S. Pyon, T. Nishizaki, Z. Shi, and T. Tamegai, Phys. Rev. B **89**, 144512 (2014).
[58] Y. Sun, Z. Shi, and T. Tamegai, Supercond. Sci. Technol. **32**, 103001 (2019).
[59] J. R. Clem and K. K. Berggren, Phys. Rev. B **84**, 174510 (2011).
[60] D. Kakehi, Y. Takahashi, H. Yamaguchi, S. Koizumi, S. Ayukawa, and H. Kitano, IEEE Trans. Appl. Supercond. **26**, 1 (2016).
[61] Y. Kakizaki, J. Koyama, A. Yamaguchi, S. Umegai, S. Ayukawa, and H. Kitano, Jpn. J. Appl. Phys. **56**, 043101 (2017).
[62] S. Ayukawa, H. Kitano, T. Noji, and Y. Koike, JPS Conf. Proc. **1**, 012123 (2014).
[63] P. J. Moll, Annu. Rev. Condens. Matter Phys. **9**, 147 (2018).

[64] See Supplemental Material at http://link.aps.org/supplemental/10.1103/PhysRevB.101.134516 for the discussion about the hysteresis loops in the *I*-*V* characteristics .

[65] M. Y. Kupriyanov and V. F. Lukichev, Fiz. Nizk. Temp. **6**, 445 (1980) [Sov. J. Low Temp. Phys. **6**, 210 (1980)].

[66] T. Kubo, Phys. Rev. Res. **2**, 013302 (2020).

[67] F. Chen, B. Zhou, Y. Zhang, J. Wei, H.-W. Ou, J.-F. Zhao, C. He, Q.-Q. Ge, M. Arita, K. Shimada, H. Namatame, M. Taniguchi, Z.-Y. Lu, J. Hu, X.-Y. Cui, and D. L. Feng, Phys. Rev. B **81**, 014526 (2010).

[68] L. Zhang, D. J. Singh, and M. H. Du, Phys. Rev. B **79**, 012506 (2009).